OPTIMIZED DESIGN OF A C-BAND 100 MeV ELECTRON LINAC FOR FLASH RADIOTHERAPY

S. Farina*, S. Akbar, R. Boldrini, E. Chiadroni, M. Coppola, A. Curcio, G. Francosioni, L. Frassi, L. Giuliano, M. Magi, M. Migliorati, A. Mostacci, L. Palumbo, V. Patera, A. Sarti
Sapienza University of Rome, Rome, Italy
D. Alesini, F. Cardelli, L. Faillace, Istituto Nazionale di Fisica Nucleare, LNF, Italy
L. Ficcadenti, Istituto Nazionale di Fisica Nucleare, Sezione di Roma I, Rome, Italy
G. Mauro, G. Torrisi, Istituto Nazionale di Fisica Nucleare, LNS, Italy

Abstract

Electron linacs are key tools for radiotherapy. Conventional low-energy linacs can treat only superficial tumors. The use of Very High Energy Electrons (VHEE, >100 MeV) enables treatment of deep-seated tumors. Furthermore, electrons are well-suited for delivering Ultra-High Dose Rates (UHDR) required for FLASH therapy, which improves healthy-tissue sparing. Combining VHEE and FLASH in a hospital environment represents an important step forward for radiotherapy. In the context of the SAFEST project at Sapienza, this work presents a compact and cost-effective accelerator layout capable of delivering hundreds of nC at 100 MeV across tens of pulses within a 100 ms irradiation window. The design emphasizes efficient RF power usage through high-efficiency C-band structures and a pulse compressor. Beam dynamics simulations and low-power RF tests validate the conceptual design. A strong focus is placed on flattening the compressed RF pulse, which must remain flat over a 1 µs interval to accelerate electrons emitted by the thermionic gun, a compact and economical source for this accelerator. The resulting 3 m linac, powered by a single 20 MW klystron, shows strong potential for future hospital-based FLASH VHEE treatments.

INTRODUCTION

Medical accelerators must be compact, cost-effective, and suitable for hospital integration. VHEE (E > 100 MeV) and UHDR operation can improve the treatment of deep-seated tumors and enhance tissue sparing [1, 2] through the FLASH effect. Radio Frequency (RF) accelerators currently represent the most reliable technology for this purpose [3, 4]. Standard S-band structures lead to excessive footprints for a clinical accelerator with E > 100 MeV, while X-band systems require strict tolerances and expensive components. The C-band (5.712 GHz, $E_{acc} \approx 50\,\mathrm{MV\,m^{-1}}$) offers an optimal compromise between efficiency and cost-effectiveness [5]. Compact and cost-effective VHEE accelerators are not yet available in clinical environments.

A 24 MeV FLASH linac [6], currently under construction at Sapienza University, will serve as a testbed for this technology. This work presents the design of a VHEE and UHDR accelerator tailored for deep-seated tumors as a future extension of the Sapienza linac, using genetic optimization, ASTRA beam dynamics, and FLUKA dose simulations.

* stefano.farina@uniroma1.it

100 MeV COMPACT ACCELERATOR LAYOUT

A commercial 14 kV thermionic triode gun [7] generates the beam, delivering a continuous current of 285 mA with a capture efficiency of 35 % when directly installed on the first accelerating structure. This configuration ensures the capture of a 100 mA bunch train.

After electrostatic acceleration, the continuous electron beam is captured, bunched, and accelerated to 4 MeV in a 22 cm standing-wave (SW) C-band injector [8], derived from the SAFEST prototype [6]. Two subsequent constant-gradient traveling-wave (TW) structures, each 1.2 m long, operate at a gradient of 40 MV m^{-1} to reach a final energy of 100 MeV. The TW cells are derived from the 24 MeV prototype.

A 20 MW klystron (5 µs pulse length, 200 Hz repetition rate), combined with a BOC-type pulse compressor, feeds the accelerating structures. The compressor design is based on the system implemented in the Sapienza prototype [9]. To deliver the required dose, the beam pulse duration must be on the order of 1 µs. High-intensity beams (100 mA) with this pulse duration induce strong beam loading effects [10], requiring dedicated RF pulse shaping. In addition, the pulse compressor response to square-like input signals is not flat, further complicating the optimization procedure.

The klystron envelope and phase modulation profile required to compensate for beam loading and properly operate the pulse compressor is therefore optimized using a multi-variable genetic algorithm. Table 1 and Fig. 1 summarize the main parameters.

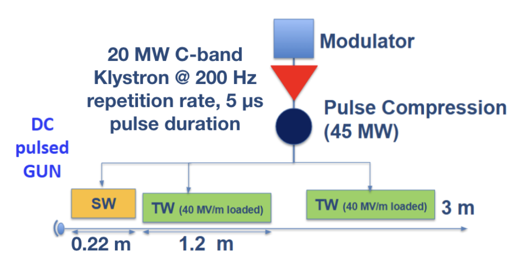

Figure 1: Layout of the compact C-band 100 MeV electron linac for FLASH radiotherapy.

Table 1: Parameters summary.

Parameter	Value
RF Frequency	5.712 GHz (C-band)
Total linac Length	3 m
Structure Configuration	SW Injector + 2 TW (CG) Sections
Final Beam Energy	100 MeV
Klystron Peak Power	20 MW
RF Pulse Length	5 µs
Repetition Rate	200 Hz
Pulse Compressor Type	BOC
Q_0 / β	10^5 / 3
Gun Type	Thermionic Triode
Extraction Voltage	14 kV
Maximum Current	1.5 A
Operating Current	100 mA
Capture Efficiency	35 %
Max Beam Pulse Duration	1 µs
Max Beam Current	100 mA
Max Charge per Pulse	100 nC
Injector Length	22 cm
Single TW Length	1.2 m
Average Gradient	40 MV m^{-1}
Shunt Impedance	100 MΩ m^{-1}
Group Velocity (in/out)	$1.75 \times 10^{-2}c$ / $0.4 \times 10^{-2}c$
Iris Radius (in/out)	6 mm / 3.5 mm

WORKING POINT

A pulse compressor is essential to reach the target energy by concentrating RF power during the beam pulse. Achieving an amplified RF profile capable of compensating for beam loading and increasing the average bunch energy requires modulation of both the klystron phase and envelope. The RF pulse is parameterized through discrete amplitude and phase values defined over a 5 µs window. The beam injection timing (T_{on}) and beam duration (T_b) are simultaneously optimized to match the compressor response. The RF envelope is constrained by a thermal limit corresponding to the energy of a non-modulated pulse. An NSGA-II algorithm [11] is used to explore different combinations of pulse parameters and beam timing. For each configuration, the full RF chain, from the klystron to the accelerating structures, is simulated and the energy gain of each bunch is evaluated. The optimization objectives are the average energy, energy spread, and total charge. The resulting optimization produces a Pareto front of non-dominated solutions. Figure 2 shows the selected working point, including the beam energy evolution and RF modulation profile.

Beam transport is validated using ASTRA [12]. A uniformly sampled bunch train is simulated, confirming stable transport along the accelerator. The transverse beam size remains well confined, with limited transverse momentum.

Due to the continuous emission within the RF bucket, a low-energy tail is transported, increasing the energy spread to 12.2 MeV (Fig. 3). However, this does not significantly affect the penetration depth in a water phantom, preserving the capability to treat deep-seated tumors, as confirmed by the dose distributions presented in the following section (Fig. 4).

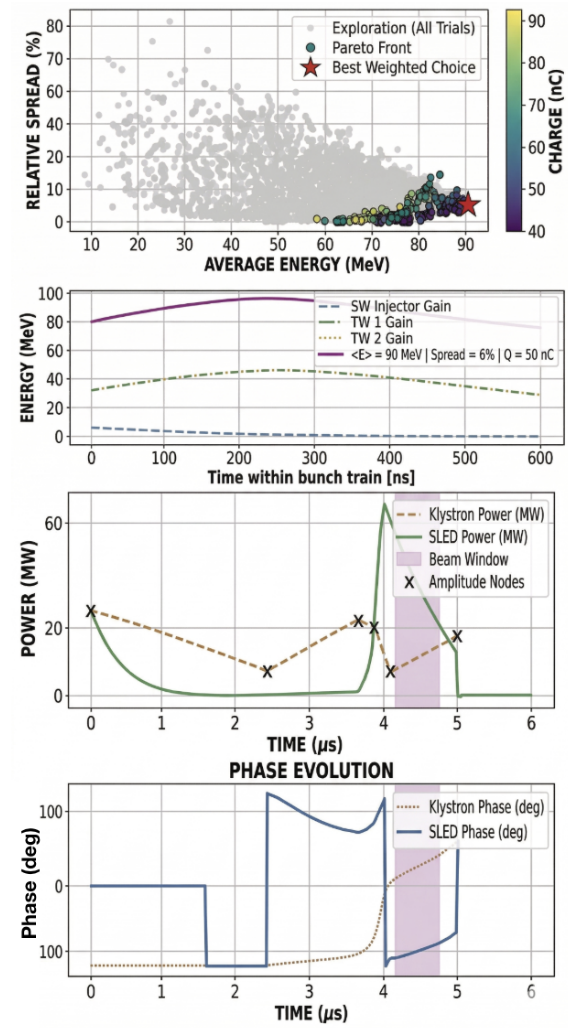

Figure 2: Pareto front metrics (top), bunch train energy (middle-top), klystron RF envelope and compressor response (middle-bottom), and phase response (bottom).

Beam Delivery and Dose Distribution

A robust delivery system must adapt the narrow linac beam to clinically relevant target volumes. Two strategies are evaluated: Wide Field and Pencil Beam Scanning, using FLUKA Monte Carlo simulations [13] for dose deposition.

Wide Field Irradiation The wide field configuration uniformly irradiates a large area (5×5 cm^2) within a single RF pulse using a 500 µm Polyether ether ketone (PEEK) scattering foil [14]. PEEK minimizes radiation-induced activation. Its radiation length (X_0 = 31.5 cm) results in only 1.6×10^{-3} of primary electron energy converting to photons, making Bremsstrahlung contributions negligible.

The 600 ns (Fig. 2) optimized pulse achieves 6 MGy s^{-1} (UHDR regime) at a depth of 15 cm in water (Fig. 4b).

Pencil Beam Scanning (PBS) Pencil beam scanning enhances spatial dose conformity by irradiating target portions

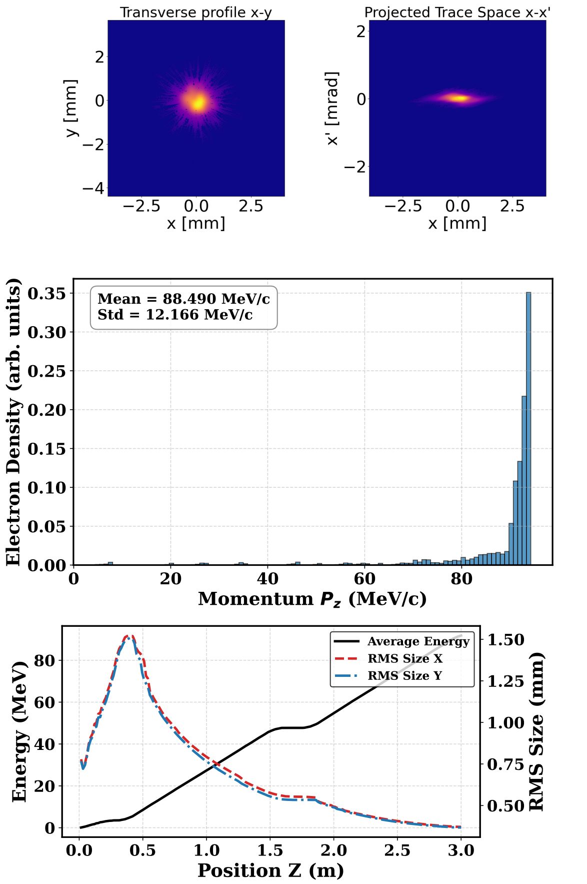

Figure 3: Exiting beam characteristics: transverse plane/trace space (top), momentum distribution (middle), and energy gain/transverse rms size (bottom).

across multiple pulses. A thinner 100 µm PEEK scatterer creates a ~ 1 cm FWHM spot size (Fig. 4c), steered dynamically by two 0.15 T ferromagnetic dipoles over a 30 cm path. A complete scan is performed using 20 pulses over 100 ms. In this configuration, both the instantaneous and average dose rates are relevant for the FLASH effect. Because the irradiated surface is smaller with respect to wide field irradiation, achieving an instantaneous UHDR requires significantly less charge. To establish an upper limit, assuming the same carried charge as the wide field configuration, the instantaneous dose rate can reach 80×10^6 Gy s^{-1} (Fig. 4d). Scaling this value by the beam duty cycle, assuming that each voxel is irradiated by only a single 600 ns pencil beam in the 100 ms, yields an average dose rate of 480 Gy s^{-1}. This confirms that the system operates well within UHDR parameters. Further studies are required to evaluate dose conformity and ensure that all target voxels receive a FLASH-level dose.

LOW POWER TEST

Low-power tests were conducted to validate the reliability of the algorithm in predicting the RF signal evolution. A Libera Low Level RF (LLRF) system and a test cavity were used for this purpose. The optimized RF modulation was generated by the LLRF system and sent to a C-band test

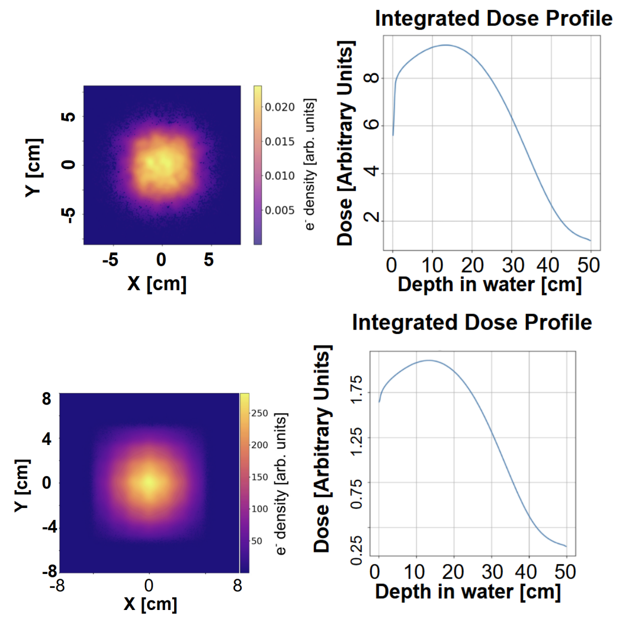

Figure 4: Delivery comparisons. Top (WF): Spatial distribution, wide field dose profile. Bottom (PBS): Spatial distribution, single pencil beam dose profile.

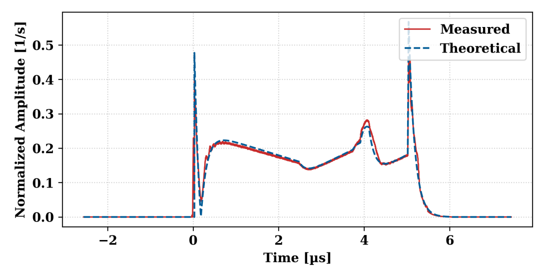

Figure 5: Comparison between measured and simulated low-power RF signals.

cavity. A directional coupler was used to send the reflected cavity signal to an oscilloscope, allowing measurement of its envelope. In this configuration, the cavity acts as a pulse compressor. The test cavity was therefore modeled in the algorithm, replacing the pulse compressor and providing a theoretical prediction of the reflected signal. Figure 5 compares the measured and simulated signals, demonstrating good agreement in the temporal evolution of the RF pulses.

CONCLUSION

This work demonstrates the feasibility of a compact 3 m VHEE FLASH electron source powered by a single 20 MW klystron. An NSGA-II optimizer was used to determine the RF modulation required to maximize the efficiency of the RF power system. Two beam delivery schemes were simulated together with dose deposition in water, demonstrating the capability to deliver UHDR at depths up to 15 cm. Low-power tests provide a preliminary validation of the RF pulse evolution computations carried out by the optimization algorithm. The SAFEST project prototype [6] will serve as an experimental platform for full validation of the proposed strategy for a VHEE FLASH linac.

REFERENCES

[1] V. Favaudon *et al.*, "Ultrahigh dose-rate FLASH irradiation increases the differential response between normal and tumor tissue in mice", *Sci. Transl. Med.*, vol. 6, p. 245ra293, 2014. doi:10.1126/scitranslmed.3008973

[2] A. Sarti *et al.*, "Deep seated tumour treatments with electrons of high energy delivered at flash rates: The example of prostate cancer", *Front. Oncol.*, vol. 11, p. 777852, 2021. doi:10.3389/fonc.2021.777852

[3] T. P. Wangler, *RF Linear Accelerators*. New Jersey, USA: Wiley, 2008. doi:10.1002/9783527623426

[4] P. B. Wilson, "High energy electron LINACs: Applications to storage ring RF system and linear collider", SLAC, Menlo Park, CA, USA, Rep. SLAC-PUB-288, 1991.

[5] L. Faillace *et al.*, "Perspectives in linear accelerator for FLASH VHEE: Study of a compact C-band system", *Phys. Med.*, vol. 104, pp. 149–159, 2022. doi:10.1016/j.ejmp.2022.10.018

[6] L. Giuliano *et al.*, "A compact C-band FLASH electron linear accelerator prototype for the VHEE SAFEST project", *Front. Oncol.*, vol. 15, p. 1516576, 2025. doi:10.3389/fonc.2025.1516576

[7] K. Masuda *et al.*, "Development of a Thermionic Triode RF Gun", in *Proc. FEL'09*, Liverpool, UK, Aug. 2009, paper TUPC18, pp. 281–284.

[8] S. V. Kustaev, "Electron bunchers for industrial linear accelerators: theory and design guide", *Eur. Phys. J. Plus*, vol. 136, p. 617, 2021. doi:10.1140/epjp/s13360-021-01312-3

[9] Z. D. Farkas *et al.*, "SLED: A method of doubling SLAC's energy", in *Proc. HEACC'74*, Stanford, CA, USA, May 1974, pp. 576–583.

[10] A. Lunin *et al.*, "Analytical solutions for transient and steady-state beam loading in arbitrary travelling wave accelerating structures", *Phys. Rev. Spec. Top. Accel. Beams*, vol. 14, p. 052001, 2011. doi:10.1103/PhysRevSTAB.14.052001

[11] K. Deb *et al.*, "A Fast and Elitist Multiobjective Genetic Algorithm: NSGA-II", *IEEE Trans. Evol. Comput.*, vol. 6, no. 2, pp. 182-197, 2002. doi:10.1109/4235.996017

[12] *A Space Charge Tracker Algorithm*, DESY, Hamburg, Germany, 2011.

[13] G. Battistoni *et al.*, "Overview of the FLUKA", *Ann. Nucl. Energy*, vol. 82, pp. 10–18, 2015. doi:10.1016/j.anucene.2014.11.007

[14] C. Robertson *et al.*, "Dual-scattering foil installation at CLEAR", in *Proc. IPAC'23*, Venice, Italy, May 2023, pp. 5059–5062. doi:10.18429/JACoW-IPAC2023-THPM073